Charge Transfer in Ferrocene-Bearing Poly(thiophene)s and Application in Organic Bilayer Photocells

Li Tan,[†] M. David Curtis,*[,†,‡] and A. H. Francis[‡]

Macromolecular Science & Engineering Center and Department of Chemistry, The University of Michigan, Ann Arbor, Michigan 48109-1055

Received December 17, 2001; Revised Manuscript Received March 19, 2002

ABSTRACT: Synthesis and characterization of poly(thiophene)s with pendant vinylene ferrocene (Fc) or cyanovinylene ferrocene units are described. Charge-transfer (CT) effects between the Fc groups and the conjugated polymer backbone have been demonstrated by the substantial photoluminescence (PL) quenching and spectroelectrochemistry. $J-V$ studies on p/n bilayer devices (ITO/polymer/perylene imide (PV)/Ag) show significant photoconductance improvement when Fc concentration reached ∼40 mol % where short-circuit current density, J_{sc}, was increased 70% as compared to a similar ITO/P3BT/PV/Ag device.

Introduction

During the past several years, the number of studies on conjugated polymers containing functional units such as metallocenes,[1,2] bipyridinium salts, and metal-coordinated macrocycles[3−5] has dramatically increased to meet the demand for new materials for photoconductors, sensor applications, and electroluminescent devices.[6,7] Recent work has shown that the electrical, optical, and electrochemical properties of these materials can vary enormously as a result of the functional groups.[8−13]

Photocells constructed with organic p/n junctions are preferred over Schottky types because of better energy-transfer efficiency.[14] Other advantages are the ease of producing pinhole-free films through two-layer processing and increased efficiency that obtains from the absorption characteristics of the device tuning over the entire visible range through a combination of materials. In organic materials, the CT (charge-transfer) states lie at higher energy than the bottom of the first excited state (S_1), and charge separation is achieved through thermal activation of CT states to the conduction level, by field-assisted dissociation of the CT states,[15,16] or by dissociation at an interface or defect (impurity).[17,18] Incorporation of functionalized ferrocene (Fc) units into polythiophenes (p-type) is an attractive possibility for enhancing the formation of CT states. Oxidation of Fc may produce further CT interactions with thiophene units that could facilitate charge separation, because it is well-known that photoexcitation of the Fc or Fc^+ group dramatically alters its redox properties.[1,2,19−21] Besides having well-known p-type character, polythiophene was chosen as the host matrix because of its easy chemical preparation/modification, good thermal stability, and excellent processability.

Research on Fc-conjugated polymer (polythiophene or polydithiafulvene) hybrid systems has been reported previously.[20,21] The Fc was conjugated in the main chain with thiophene/dithiafulvene units. The approach used in this study involves covalently attaching the Fc units as pendant groups to the conjugated polythiophenes. This approach has several benefits. First of all, the chemistry and physical properties of the parent polythiophene material are well-known as compared to a newly synthesized polymer backbone. Second, the use of other electroactive groups, such as electron-withdrawing or electron-donating groups, to attach the ferrocene can further modify the redox properties of the pendant functional units. Third, by altering the redox properties of the main chain with respect to the pendant groups, polymers with a large range of electron donor/acceptor main chain/pendant groups are easily prepared. With all these, electronic/optical properties of new materials can be investigated, and optimized properties can be reached.

In this paper, we describe the synthesis of two Fc-bearing polythiophenes. To probe the effect of tuning the electron density on the Fc group, two monomers were synthesized via Knoevenagel base condensation or Wittig reaction (Scheme 1). The synthesis of all the copolymers involved a nickel-mediated coupling reaction between the functionalized monomers and brominated 3-butylthiophene (Scheme 2). Fabrication of photocells using these hybrid materials as the p-type layer demonstrated interesting optoelectrical properties as a function of the iron centers.

Experimental Section

Materials. All manipulations and polymerizations were performed under a nitrogen atmosphere using standard Schlenk line techniques unless otherwise stated. Reagents were purchased and used as received unless otherwise stated.

^{1}H NMR spectra were collected on a Varian 300 or 400 MHz spectrometer and referenced to the residual proton solvent resonance. GC-MS data were collected on a Finnigan model 4500 spectrometer. UV−vis spectra were collected on a Shimadzu 3101PC with baseline correction. Near-IR (NIR) spectra were collected on a Perkin-Elmer 2000 with background correction. Emission spectra were collected on a Fluoro-Max2 interfaced with a PC. TGA was performed on a Perkin-Elmer TGA 7 with 5−15 mg of powdered sample at scan rate of 40 °C/min under nitrogen or air. Molecular weights were determined on a Waters GPC with methylene chloride as the eluent and polystyrene standards. Elemental analyses were performed by the Microanalysis Laboratory, Department of Chemistry, The University of Michigan. Cyclic voltammetry was performed with a three-electrode potentiostat designed

[†] Macromolecular Science & Engineering Center.
[‡] Department of Chemistry.

10.1021/ma012183v CCC: $22.00
Published on Web 05/10/2002

Scheme 1. Synthesis of Monomers 1 and 2

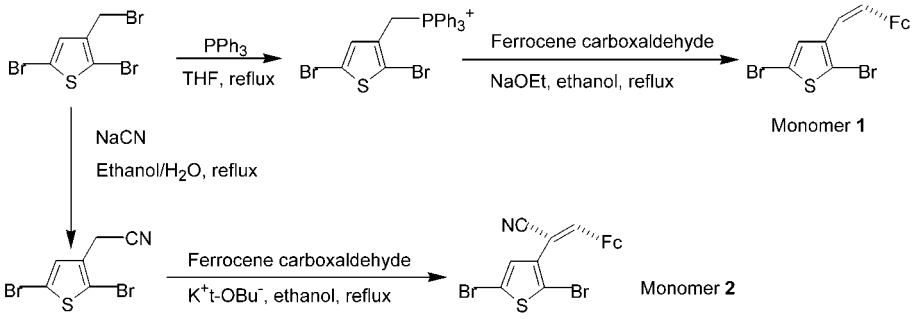

Scheme 2. Copolymerization via Ni(0)-Mediated Coupling

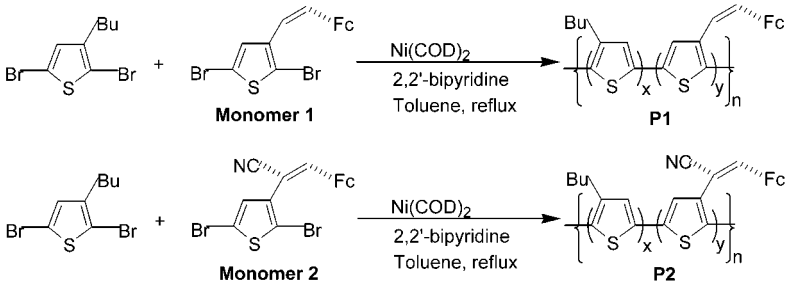

and built by Wayne Burkhardt (University of Michigan, Department of Chemistry Electronics Shop) interfaced with a PC running a custom software program written by Dr. Steven Parus (University of Michigan, Department of Chemistry). The computer drives the voltage ramp and collects the current−voltage data. The electrolyte was 0.1 M tetrabutylammonium hexafluorophosphate ($TBAPF_6$) in dried acetonitrile; the working and auxiliary electrodes were platinum, and the reference electrode was 0.01 M $Ag/AgNO_3$ in addition to the 0.1 M $TBAPF_6$ in acetonitrile. Thin films of polymers for conductivity measurement were made by solvent casting. The film thickness was measured by a Sloan Dektak-3 surface profilometer.

3-Butylthiophene.[22] A clear liquid (75.0% yield) was received after distillation at 65 °C under 10 mmHg. ^{1}H NMR ($CDCl_3$): δ 0.90 (t, 3H), 1.12−1.85 (m, 4H), 2.65 (t, 2H), 6.95 (m, 2H), 7.28 (d, 1H).

2,5-Dibromo-3-butylthiophene.[22] A reddish liquid (50.0% yield) was received after distillation at 65 °C under 0.01 mmHg. ^{1}H NMR ($CDCl_3$): δ 0.90 (t, 3H), 1.12−1.85 (m, 4H), 2.65 (t, 2H), 6.87 (s, 1H). GC-MS: 99.5% purity was measured.

2,5-Dibromo-3-methylthiophene.[22] A clear liquid (92.0% yield) was received after distillation at 105−108 °C under 17 mmHg. ^{1}H NMR ($CDCl_3$): δ 2.13 (s, 3H), 6.75 (s, 1H). GC-MS: 92.0% purity was determined.

2,5-Dibromo-3-(bromomethyl)thiophene.[23] A clear liquid (50% yield) was received after distillation at 85 °C under 0.08 mmHg. ^{1}H NMR ($CDCl_3$): δ 4.23 (s, 2H), 6.87 (s, 1H).

2,5-Dibromo-3-(triphenylphosphinomethyl)thiophene Bromide (Ylide). A 250 mL Schlenk flask equipped with an addition funnel and stir bar was charged with 2,5-dibromo-3-bromomethylthiophene (3.0 mmol, 1.0 g) in anhydrous THF (20 mL). A triphenylphosphine (3.0 mmol, 0.78 g) solution in THF (20 mL) was added dropwise over 20 min. The temperature was raised until reflux, causing the clear pink solution to turn cloudy right away. After refluxing overnight, the mixture was cooled to room temperature. The precipitate was filtered off and washed with ether. A white powder was collected (1.25 g, 70% yield). ^{1}H NMR ($CDCl_3$): δ 5.44 (d, J = 14.0 Hz, 2H), 6.86 (s, 1H), 7.60−7.78 (m, 15H). Melting point: 220−221 °C.

1-(2,5-Dibromothiophene-3-yl)-2-ferrocenylethene (Monomer 1). A 250 mL Schlenk flask equipped with a water condenser and stir bar was charged with the above ylide (4.02 mmol, 2.4 g), ferrocene carboxyaldehyde (4.02 mmol, 0.86 g), and potassium *tert*-butoxide (4.20 mmol, 0.47 g) in ethanol (40 mL). The solution was allowed to reflux overnight. After cooling to room temperature, the mixture was added to H_2O (100 mL), and the mixture was then extracted with CH_2Cl_2 (3 × 100 mL). The CH_2Cl_2 extracts were combined and dried over $MgSO_4$; then the solvent was removed by rotary evaporation. The resulting oil was run through a silica column (hexane eluent). Clear oil with *E*- and *Z*-ratio of 60/40 was collected. ^{1}H NMR ($CDCl_3$) for *E*: δ 4.07 (s, 5H), 4.24 (t, J = 1.8 Hz, 2H), 4.38 (t, J = 1.8 Hz, 2H), 6.49 (d, J = 16.1 Hz, 1H), 6.62 (d, J = 16.1 Hz, 1H), 7.09 (s, 1H). ^{1}H NMR ($CDCl_3$) for *Z*: δ 4.06 (s, 5H), 4.13 (t, J = 1.8 Hz, 2H), 4.24 (t, J = 1.8 Hz, 2H), 5.99 (d, J = 11.7 Hz, 1H), 6.35 (d, J = 11.7 Hz, 1H), 6.87 (s, 1H). λ_{max}(abs) = 310, 370, and 450 nm (CH_2Cl_2).

Poly(3-butylthiophene-*co*-(3-(2-ferrocen-1-yl-vinyl)thiophene)) (P1-10). A dry 100 mL Schlenk flask equipped with a water condenser, stir bar, and N_2 inlet was charged with monomer **1** (0.40 mmol, 0.18 g), 2,5-dibromo-3-butylthiophene (4.0 mmol, 1.19 g), $Ni(COD)_2$ (4.50 mmol, 1.24 g), and 2,2′-bipyridyl (4.5 mmol, 0.72 g) in anhydrous toluene (50 mL). The reaction mixture was heated to reflux overnight. The dark brown, viscous mixture was precipitated into acidic MeOH (300 mL). The solid was collected by filtration and then dissolved in chloroform. After filtering through a $^1/_4$ in. plug of Celite, the filtrate was concentrated by rotary evaporation and reprecipitated into methanol. An orange solid was collected and dried under vacuum (0.25 g, 37.9% yield). ^{1}H NMR ($CDCl_3$): δ 6.8−7.2 (1H, thiophene-ring proton), 4.0−4.5 (1H, ferrocene ring protons), 2.4−2.9 (2H, α-methylene protons), 1.2−1.9 (4H, β- and γ-methylene protons), 0.6−0.9 (3H, methyl protons). λ_{max}(abs) = 410 nm, 318 nm (CH_2Cl_2); 405 nm, 320 nm (film). λ_{max}(em) = 545 nm (CH_2Cl_2). λ_{max}(ex) = 370−438 nm (CH_2Cl_2). Near-IR: λ_{max}(abs) = 813 and 1730 nm (I_2-doped film). M_n = 45 400, M_w = 210 000, PDI = 4.63. Anal. Calcd for **P1-10**: C, 68.84; H, 6.65; S, 20.86. Found: C, 67.67; H, 6.58; S, 19.93. TGA analysis (N_2): 5% weight loss at 426 °C; 40% weight loss at 515 °C.

P1-20. The same procedure and workup were followed as described above, except the ferrocene-bearing monomer was used in 20% mole ratio. An orange powder was collected (87.1% yield). ^{1}H NMR ($CDCl_3$): δ 6.8−7.2 (1H, thiophene-ring proton), 4.0−4.5 (2H, ferrocene ring protons), 2.4−2.9 (2H, α-methylene protons), 1.2−1.9 (4H, β- and γ-methylene protons), 0.6−0.9 (3H, methyl protons). λ_{max}(abs) = 415 nm, 318 nm (CH_2Cl_2); 420 nm, 320 nm (film). λ_{max}(em) = 540 nm (CH_2Cl_2). λ_{max}(ex) = 376−400 nm (CH_2Cl_2). Near-IR: λ_{max}(abs) = 837 nm, 1736 nm (I_2-doped film). M_n = 48 300, M_w = 223 000, PDI = 4.62. Anal. Calcd for **P1-20**: C, 69.65; H, 6.29; S, 19.49;

Fe, 5.80. Found: C, 63.26; H, 6.18; S, 16.26; Fe, 5.80. TGA analysis (N_2): 5% weight loss at 400 °C; 40% weight loss at 535 °C.

P1-40. The same procedure and workup were followed as described above, except the ferrocene-bearing monomer was used in 40% mole ratio. An orange solid was collected (93.4% yield). ^{1}H NMR ($CDCl_3$): δ 6.8−7.2 (1H, thiophene-ring proton), 4.0−4.5 (5.2H, ferrocene ring protons), 2.4−2.9 (2H, α-methylene protons), 1.2−1.9 (4H, β- and γ-methylene protons), 0.6−0.9 (3H, methyl protons). λ_{max}(abs) = 420 nm, 315 nm (CH_2Cl_2); 440 nm, 320 nm (film). λ_{max}(em) = 535 nm (CH_2Cl_2). λ_{max}(ex) = 377−405 nm (CH_2Cl_2). Near-IR: λ_{max}(abs) = 825 nm, 1675 nm (I_2-doped film). M_n = 12 300, M_w = 96 000, PDI = 7.84. Anal. Calcd for **P1-40**; C, 67.48; H, 5.54; S, 16.53. Found: C, 60.20; H, 4.98; S, 12.93. TGA analysis (N_2): 5% weight loss at 398 °C; 40% weight loss at >800 °C. TGA analysis (air): calcd: 85% weight loss; found: 78% weight loss at >720 °C.

2,5-Dibromo-3-(cyanomethyl)thiophene. A 250 mL Schlenk flask equipped with a stir bar and N_2 inlet was charged with sodium cyanide (36 mmol, 1.75 g) and 2,5-dibromo-3-(bromomethyl)thiophene (30 mmol, 10.0 g) in an ethanol/water mixture (1:1, 30 mL). The reaction was allowed to run overnight under reflux. After cooling, the mixture was extracted with CH_2Cl_2 (3 × 100 mL) and dried over $MgSO_4$, and the solvent was removed by rotary evaporation. After running through a column (hexane eluent), an oil-like product was collected (8.03 g, 85.9% yield). ^{1}H NMR ($CDCl_3$): δ 3.54 (s, 2H), 6.95 (s, 1H). GC-MS: 281 (M+).

2-(2,5-Dibromothiophene-3-yl)-3-ferrocenylacrylonitrile (Monomer 2). A 250 mL Schlenk flask equipped with a water condenser, stir bar, and N_2 inlet was charged with 2,5-dibromo-3-(cyanomethyl)thiophene (3.57 mmol, 1.0 g), ferrocene carboxyaldehyde (3.93 mmol, 0.84 g), and potassium *tert*-butoxide (4.40 mmol, 0.50 g) in a THF/ethanol (4:1, 50 mL) mixture. The reaction was allowed to reflux for 7 h. The mixture was poured over crushed ice and extracted with $CHCl_3$ (3 × 100 mL), and the extract was dried over $MgSO_4$. After rotary evaporation, the residue was run through a column (1:1 CH_2Cl_2/hexane). An oily product was recovered (0.72 g, 40.0% yield). ^{1}H NMR ($CDCl_3$) showed mixture of *E*- and *Z*-products: δ 4.19 (s, 5H), 4.50 (s, 2H), 4.86 (s, 2H), 6.96 (s, 1H), 7.24 (s, 1H); δ 4.17 (s, 5H), 4.48 (s, 2H), 4.84 (s, 2H), 7.13 (s, 1H), 7.25 (s, 1H). λ_{max}(abs) = 330 nm, 500 nm (CH_2Cl_2).

Poly(3-butylthiophene-*co*-(3-(1-cyano-2-ferrocen-1-ylvinyl)thiophene)) (P2-10). A dry 100 mL Schlenk flask equipped with a water condenser, stir bar, and N_2 inlet was charged with monomer **2** (0.40 mmol, 0.19 g), 2,5-dibromo-3-butylthiophene (4.0 mmol, 1.19 g), $Ni(COD)_2$ (5.50 mmol, 1.51 g), and 2,2′-bipyridyl (5.5 mmol, 0.89 g) in anhydrous toluene (50 mL). The reaction mixture was heated to reflux overnight. The viscous mixture was precipitated into methanol (300 mL). The solid was filtered off, dissolved in chloroform, and then concentrated by rotary evaporation. The polymer was reprecipitated in methanol. An orange solid was collected and dried under vacuum (0.16 g, 23.7% yield). ^{1}H NMR ($CDCl_3$): δ 6.8−7.2 (1H, thiophene-ring proton), 4.0−5.0 (0.87H, ferrocene ring protons), 2.4−2.9 (2H, α-methylene protons), 1.2−1.9 (4H, β- and γ-methylene protons), 0.6−0.9 (3H, methyl protons). λ_{max}(abs) = 390 nm, 330 nm (CH_2Cl_2); 400 nm (film). λ_{max}(em) = 544 nm (CH_2Cl_2). λ_{max}(ex) = 371−430 nm (CH_2Cl_2). Near-IR: λ_{max}(abs) = 811 nm, 1668 nm (I_2-doped film). M_n = 16 000, M_w = 35 000, PDI = 4.52. Anal. Calcd for **P2-10**: C, 68.62; H, 6.56; N, 0.80; S, 20.81. Found: C, 63.23; H, 6.61; N, 0.79; S, 18.00. TGA analysis (N_2): 5% weight loss at 408 °C; 40% weight loss at 517 °C.

P2-20. The same procedure and workup were followed as described above, except the ferrocene-bearing monomer was used in 20% mole ratio. An orange solid was collected (55% yield). ^{1}H NMR ($CDCl_3$): δ 6.8−7.2 (1H, thiophene-ring proton), 4.0−5.0 (1.7H, ferrocene ring protons), 2.4−2.9 (2H, α-methylene protons), 1.2−1.9 (4H, β- and γ-methylene protons), 0.6−0.9 (3H, methyl protons). λ_{max}(abs) = 400 nm, 325 nm (CH_2Cl_2); 391 nm, 328 nm (film). λ_{max}(em) = 544 nm (CH_2Cl_2). λ_{max}(ex) = 372−415 nm (CH_2Cl_2). Near-IR: λ_{max}(abs) = 805 nm, 1729 nm (I_2-doped film). M_n = 10 000, M_w = 76 000, PDI = 7.48. Anal. Calcd for **P2-20**: C, 67.98; H, 6.10; N, 1.34; S, 19.20. Found: C, 62.77; H, 6.24; N, 1.16; S, 16.68. TGA analysis (N_2): 5% weight loss at 409 °C; 40% weight loss at 600 °C.

P2-40. The same procedure and workup were followed as described above, except the ferrocene-bearing monomer was used in 40% mole ratio. An orange solid was collected (83% yield). ^{1}H NMR ($CDCl_3$): δ 6.8−7.2 (1H, thiophene-ring proton), 4.0−5.0 (4.5H, ferrocene ring protons), 2.4−2.9 (2H, α-methylene protons), 1.2−1.9 (4H, β- and γ-methylene protons), 0.6−0.9 (3H, methyl protons). λ_{max}(abs) = 380 nm, 325 nm (CH_2Cl_2); 328 nm, 477 nm (film). λ_{max}(em) = 539 nm (CH_2Cl_2). λ_{max}(ex) = 375 nm, 415 nm (CH_2Cl_2). Near-IR: λ_{max}(abs) = 762 nm, 1346 nm (I_2-doped film). M_n = 22 000, M_w = 112 000, PDI = 5.19. Anal. Calcd for **P2-40**: C, 66.63; H, 5.12; N, 2.48; S, 15.82. Found: C, 62.57; H, 5.62; N, 2.32; S, 13.61. TGA analysis (N_2): 5% weight loss at 342 °C; 40% weight loss at >800 °C. TGA analysis (air): calcd 86% weight loss; found 82% weight loss at >650 °C.

Spectroelectrochemistry Measurement. Polymers (**P1-20** and **P2-20**) were cast onto ITO (indium−tin oxide) slides to form the transparent brown film. ITO served as the working electrode, Ag wire for the reference, and Pt wire for the counter electrode. All the electrodes were connected to a potentiostat, and the experiments were performed in a UV cell containing 0.1 M tetrabutylammonium hexafluorophosphate ($TBAPF_6$) electrolyte in acetonitrile for UV−vis spectroscopy measurement. Cell potentials were held for 1 min at 0.4 V for **P1-20**, 0.55 V for **P2-20**, and 1.2 V for both polymers. After the oxidation, a zero potential was applied to reduce the materials. The UV−vis spectra were monitored after both oxidation and reduction events.

Device Fabrication and Characterization. Diode structures consisting of p/n bilayers, **P3BT/PV**, **P1-#/PV,** and **P2-#/PV** (**# = 10**, **20**, and **40**) sandwiched between ITO on glass (Delta Technology, 15Ω/□) and evaporated Ag electrodes were fabricated. Uniform polymer films were deposited by spin-coating polymer solutions in chloroform (10−25 mg/mL). **PV** was deposited to a thickness of 50−100 nm by vacuum evaporation. The deposition rate was 25 Å/s at a pressure of 10^{-6}−10^{-5} Torr. The average device area was 0.25 cm^2. A Keithley 617 electrometer with a PCI-GPIB card was used to collect $J-V$ data and action spectra measurements. A GCA/McPherson ($^1/_4$ m *f*/9) monochromator with 4 nm band-pass was used to provide monochromatic light in order to record the diode response under specific wavelength excitation.

Results and Discussion

Synthesis. The precursors of the monomers were all derivatives of 2,5-dibromo-3-bromomethylthiophene, which provided a convenient building block to tailor functional monomers in which the Fc group was attached to the thiophene ring via a vinylene or a cyanovinylene group. The cyano group was integrated into the monomer **2**, with the hope of increasing the electron-withdrawing ability of the Fc pendant group in order to adjust the electronic communication between the metal centers and the conjugated ring system. Knoevenagel base condensation and the Wittig reaction were used to make the two Fc-bearing thiophene monomers (Scheme 1).

Polymerizations (Scheme 2) gave well-defined polymers (**P1** and **P2**). Copolymerization between butylthiophene and Fc units will produce four different diad configurations for the α-methylene ^{1}H resonance. However, only two different chemical shifts were observed at δ = 2.65 and 2.42 in **P1** and at δ = 2.68 and 2.44 in **P2** (Figure 1), which in position are similar to the HH and HT α-methylene chemical shifts in the homopolymer, P3BT.[24,25] If the NMR chemical shift is not very sensitive to the nature of the pendant group, then the

Table 1. Synthesis and Physical Properties of Copolymers

copolymer	Fc, mol % initial	Fc, mol % obtained[a]	reaction time, days	% yield	M_n	M_w	PDI
P1-10	10.0	10.0	1	38	45 400	210 000	4.63
P1-20	20.0	17.0	1	87	48 300	223 000	4.62
P1-40	40.0	36.1	1	93	12 300	96 000	7.84
P2-10	10.0	8.8	2	23	35 000	16 000	4.52
P2-20	20.0	16.0	1	55	10 000	76 000	7.48
P2-40	40.0	35.9	3	83	22 000	112 000	5.19

[a] Estimated according to ^{1}H NMR.

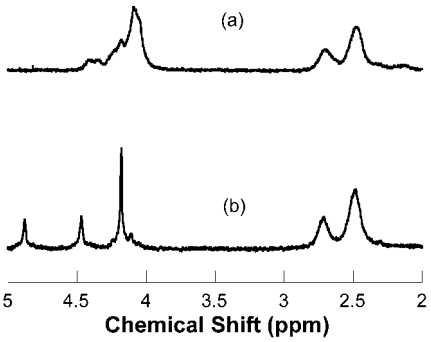

Figure 1. ^{1}H resonance of protons on ferrocene and α-methylene group: (a) **P1-20;** (b) **P2-20**.

lower field resonance would be assigned to the HT diad and the higher field peak to the HH. However, this puts the HT content at less than 50%, i.e., an apparent selectivity toward a HH−TT structure. This does not make much sense from a steric viewpoint and from the fact that Ni(0) coupling of dibromides usually gives an excess of HT diads. Hence, it is likely that the low field resonance is the HT (Bu−Bu) diad, and the remaining three diads resonate at the higher field position. In addition, protons on the Fc ring were seen as broad peaks in the **P1** series and rather sharp ones in the **P2** series in the range 4.0−5.0 ppm. The cyano group was successfully incorporated into the **P2** series as evidenced by 2206 cm^{-1} $\nu_{C\equiv N}$ vibration in the FT-IR spectrum. The ratio of monomers in the final polymer was nearly the same as the ratio in the initial feed. It has been our experience with Ni(0) coupling reactions that this is not the case when the reactivity of the monomers are different. In this case, one could reasonably expect the reactivities of the C−Br bonds of the different monomers to be similar, and if the reactivities are similar, then random copolymers result from the Ni(0) coupling. The actual concentration of the Fc groups was determined by the integration ratio of the Fc ^{1}H resonance to the resonance of the terminal methyl group on butylthiophene (Table 1). Elemental analysis showed significantly lower percentages of carbon and sulfur compared to the calculated amount. We believe the low analysis is due to reactions between iron with these elements during the combustion, forming iron carbides and iron sulfate. This hypothesis is supported by (a) atomic absorption detection of the iron concentration in **P1-20** ($Fe_{calcd} = Fe_{found} = 5.80$ by Chemisar Lab. Inc.) and (b) the significant ash residue left in the TGA analysis under both nitrogen and air observed for **P1-40** and **P2-40**. Furthermore, ^{1}H NMR spectra were consistent with pure polymers as formulated.

Optical Properties. The incorporation of Fc into the poly(3-butylthiophene)s affected the spectral properties. Figure 2 showed the UV−vis spectra of solutions of these copolymers. The peak at 295 eV (420 nm) represents the absorption of butylthiophene main chain,

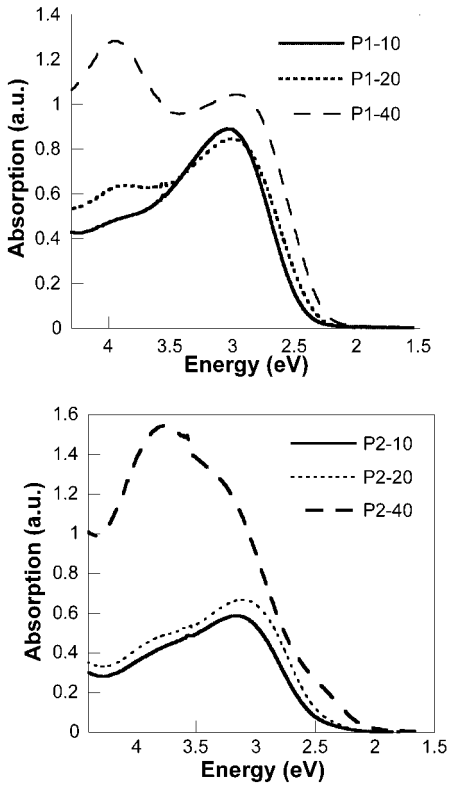

Figure 2. UV−vis of copolymers in CH_2Cl_2: (top) **P1** series; (bottom) **P2** series.

which is similar to the absorption of the parent poly(3-butylthiophene).[25] Furthermore, the peak at 2.95−3.10 eV (400−420 nm) shifts to longer wavelength as (a) the concentration of Fc group increases and (b) on going from solution to solid state. The latter behavior is characteristic of the $\pi-\pi^*$ transition of P3ATs. The fact that the peak maximum, as well as the solution → solid-state shift, also red shifts with increasing concentration of Fc groups suggests that the HT content increases as more Fc groups are incorporated. An increase in HT content might alleviate steric congestion as the concentration of Fc groups increases. The peak near 4.0 eV (310 nm) (**P1**) or 3.76 eV (330 nm) (**P2**) arises from a MLCT band associated with the aryl-substituted Cp ligand.[2,26] The "band II" d → d transition of the Fc group, usually found in the 2.5−3.0 eV (400−500 nm) range, is simply buried by the much more intense, symmetry allowed $\pi-\pi^*$ transition of the poly(thiophene) chain. Thus, the position of the 310−330 nm peak is insensitive to the concentration of Fc units in the polymer and is also unaffected on going from solution to solid state. The intensity of this peak, however, is linearly related to the Fc concentration (Figure 3), as expected. This verifies that the Fc concentration was well controlled.

NIR spectra of the doped polymer films (exposed to I_2 vapor for 7 h) are shown in Figure 4. Two new broad

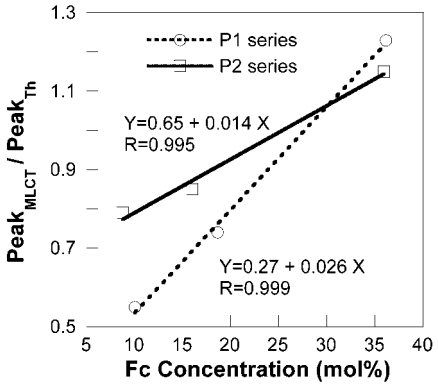

Figure 3. Relationship between the absorption ratio of MLCT and butylthiophene units ($peak_{MLCT}/peak_{Th}$) on UV−vis with Fc concentration.

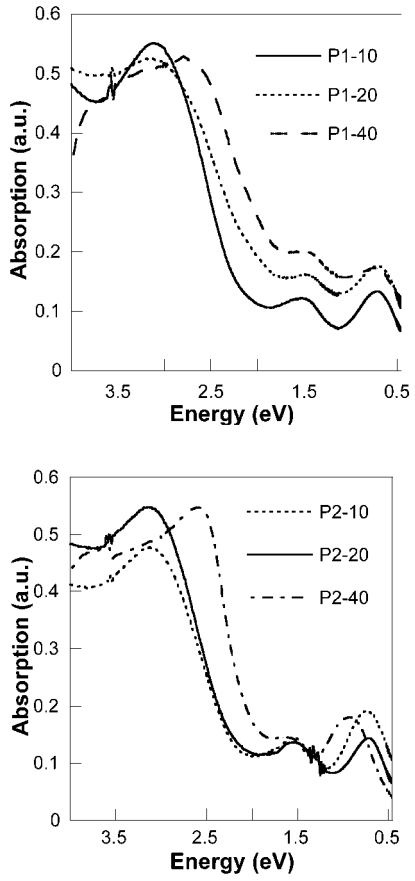

Figure 4. NIR spectra of doped copolymers: (top) **P1** series; (bottom) **P2** series.

peaks around 1.6−1.5 eV (700−840 nm) and 1.0−0.7 eV (1600−1750 nm) appeared in the doped samples. These peaks have been assigned previously to absorptions of polarons and bipolarons,[27] but an alternate model suggests these peaks arise from the band structure associated with the HOMO → LUMO, HOMO → LUMO+1, HOMO-1 → LUMO, and HOMO-1 → HOMO transitions.[28] However, CT bands between the thiophene and Fc^+ groups are also expected to be in this region. While it is impossible to make definitive assignments without further work, we note that the CT bands associated with the Fc units are likely to be much less intense (ϵ < 2000) than the strong bands shown in Figure 4. The conductivities of these doped films are in the semiconductor range ($(0.2-1) \times 10^{-3}$ S/cm) and are similar to those of the parent P3BT polymers.

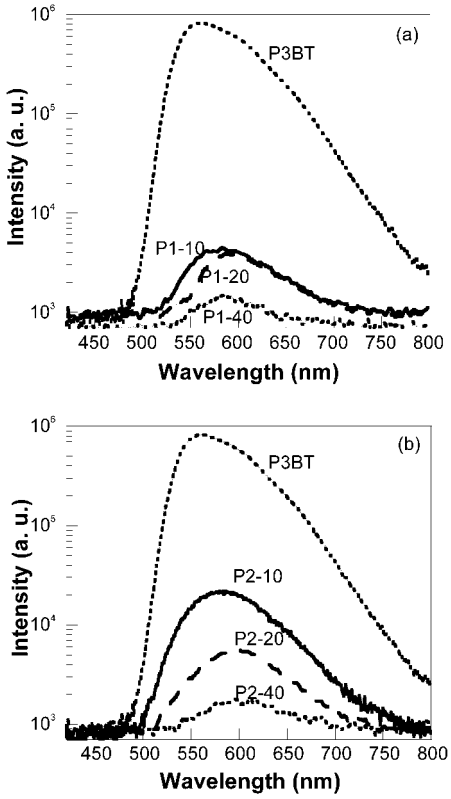

Figure 5. PL quenching of polymers in CH_2Cl_2: (a) **P1** series; (b) **P2** series. The concentration of the thiophene units was kept at 1.0×10^{-7} M.

More interesting are the photoluminescent properties of these polymers**.** Attachment of Fc units to the P3BT chain caused a dramatic quenching of photoluminescence in solution as shown in Figure 5. The concentrations of the thiophene ring were kept the same in these two copolymer series for this measurement. This phenomenon suggests that charge transfer (CT) occurs between the Fc units and the conjugated thiophene rings. In this case, Fc can donate an electron into the half-occupied HOMO of the thiophene after the electron in the HOMO is excited into the LUMO, thus forming Fc^+ and negatively charged thiophene. Charge recombination between the Fc^+ ion and the electrons from the excited state of the thiophene leads to nonluminescent decay of the initially formed S_1 state:

$$P^0 + h\nu \rightarrow P^* \quad \text{exciton formation}$$

$$P^* + Fc^0 \rightarrow P^- + Fc^+ \quad \text{charge-transfer}$$

$$P^- + Fc^+ \rightarrow P^0 + Fc^0 + \text{heat} \quad \text{nonluminescent decay}$$

However, Förster transfer is another possibility for this quenching.[29] The quantum yield for fluorescence will decrease by exciton transfer to the Fc units because the excited Fc* undergoes rapid intersystem crossing to nonradiative triplet states:

$$P^0 + h\nu \rightarrow P^* \quad \text{exciton formation}$$

$$P^* + Fc^0 \rightarrow P^0 + Fc^* \quad \text{Förster transfer}$$

$$Fc^* \rightarrow Fc^0 + \text{heat} \quad \text{nonluminescent decay}$$

where P stands for the thiophene unit on the polymer and Fc stands for the ferrocene unit.

Table 2. Optical Bandgap, Oxidation Potential of P1 and P2, and Device Properties of Bilayer Devices

copolymer	E_g (eV)[a]	$E_1^{1/2}$ (V)[b]	$E_2^{1/2}$(V)[b]	J_{sc} (nA)[d]	V_{oc} (V)[d]	FF[d]
P1-10	2.48	−0.02	+0.48	4.8	0.25	0.28
P1-20	2.38	−0.03	+0.40	2.8	0.20	0.30
P1-40	2.25	−0.03	+0.41	340	0.22	0.34
P2-10	2.50	+0.09	+0.44	8.6	0.17	0.27
P2-20	2.48	+0.14	+0.41	1.8	0.11	0.31
P2-40	2.14	+0.13	*c*	12	0.22	0.32

[a] Band gap was extrapolated from the low energy edge of the maximum absorption to the baseline edge. [b] Oxidation potential was referenced to the ferrocene/ferrocenium couple (E^o = 0.40 vs SHE). [c] Obscured by the huge ferrocene oxidation peak. [d] Exposed to 3.8 mW/cm^2 white light. ITO/polymer/PV/Ag structure was used. V_{oc} = open-circuit voltage, J_{sc} = short-circuit current density, FF = fill factor. For P3BT/PV, J_{sc} = 200 nA, V_{oc} = 0.50 V, FF = 0.34.

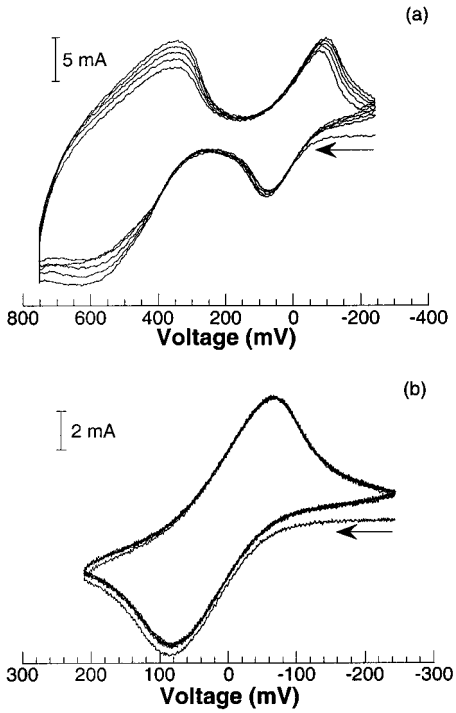

Figure 6. Cyclic voltammetry of **P1-10** in THF−$TBAPF_6$: (a) oxidation to +800 mV; (b) oxidation of ferrocene unit only. Scan rate: 100 mV/s. Ref. to Fc/Fc^+.

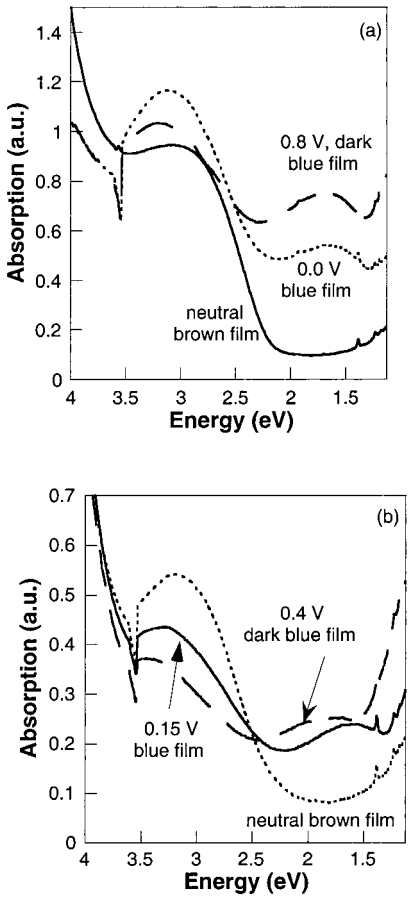

Figure 7. Oxidation of polymer films in CH_3CN (0.1 M CH_3CN−$TBAPF_6$ as electrolyte): (a) **P1-20**; (b) **P2-20**.

Electrochemistry. (All the data were referenced to the Fc/Fc^+ couple, with E_{ox} set to 0.0 V. To convert to NHE, add 0.40 V to the reported potentials.) Two oxidation potentials were found in the solution cyclic voltammetry (CV) of these copolymers. The voltammogram is characteristic of redox reversible electroactive species, with rather unsymmetrical shapes but equal heights of anodic and cathodic peaks, as shown in Figure 6 for **P1-10**. The reversible peak at 0.4−0.48 V was due to the oxidation of thiophene ring while the peak at 0.0−0.14 V was from the oxidation of Fc in the copolymer. The substitution of a cyano group on the vinyl group shifted the oxidation of Fc to higher value, 0.08−0.14 V, due to the strong electron-withdrawing ability of the cyano group. As indicated by Table 2, oxidation potentials of Fc and thiophene rings stay rather constant with the change in Fc concentration.

Spectroelectrochemistry. Figures 7 and 8 show the in situ UV−vis spectra of the electrochemically oxidized/reduced polymer films. These spectra matched well with the iodine-doped polymer NIR spectra. A new broad peak appeared around 1.77 eV (700 nm) at low oxidation potential (0.0 V for **P1** and 0.15 V for **P2**) along with a tail of a new peak at E < 1.13 eV (λ_{max} > 1100 nm) at higher oxidation potential (0.80 V). The color of films changed from brown to blue, the characteristic color of the ferrocenium ion. The oxidized polymer retained some of the bluish color when reduced by application of a zero potential. This may be due to pockets of oxidized polymer being trapped in the nonconductive, reduced polymer, as can happen in the thick films used here, or it may be that some polymer decomposed at higher potentials.

From CV, both Fc and thiophene units should be oxidized with a potential of 0.8 V on the polymer films; thus, the spectra were similar to those obtained from doped polymers in the NIR. However, at a potential of 0.0−0.15 V, only Fc oxidation should occur, but characteristics of both ferrocenium ion and the doped polymer were seen in the spectra. This suggests that the Fc units on the polymers cannot be oxidized without some electron transfer from the conjugated thiophene rings, a result consistent with other published work.[21] None of the spectra returned to the original brown color or spectrum after the polymer films were oxidized and reduced.

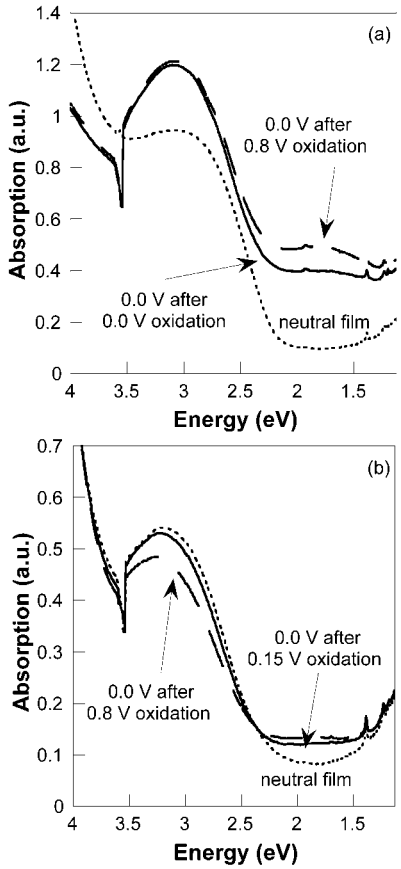

Figure 8. Reduction of oxidized polymer films in CH_3CN (0.1 M $CH_3CN-TBAPF_6$ as electrolyte): (a) **P1-20**; (b) **P2-20**.

Photodiode Properties. Organic diodes with the structure of ITO/polymer/PV/Ag were investigated. In this study, perylene-3,4,9,10-tetracarboxylic acid diimide (**PV**) was used as the n-type material.[30] The energy band structure of these functionalized polymers can be approximated by equating the HOMO and LUMO energies of P3BT to the valence and conduction band edges, respectively, with the Fc levels acting as intragap dopant levels. In a cyclic voltammogram, P3BT is oxidized at 0.4 V vs Fc/Fc^+ couple, which corresponds to an ionization energy of 5.2 eV, referenced to the vacuum level.[31] The optical band gap, $E_g = 2.5$ eV, was determined by extrapolating the optical absorption edge to the baseline ($\lambda_{edge} = 500$ nm). Thus, the LUMO energy of P3BT is estimated to lie at 2.7 eV. The energy levels of **PV** shown in Figure 9 were obtained from literature values.[32] Ohmic contacts will form on the p-side for holes ($\phi_0 = 5.2-4.8 = 0.4$ eV, Figure 9) and on the n-side for electrons. However, these contacts become Schottky type for opposite carriers, such as electron injection on the p-side ($\phi_0' = 4.8-2.7 = 2.1$ eV, blocking barrier, Figure 9) or hole injection on the n-side. The incorporation of the Fc group puts a dopant level at 4.77−4.79 eV for **P1** and 4.88−4.94 eV for **P2**. $J-V$ curves (photoexcited through ITO side) of the devices are shown in Figure 10. Diode behavior was observed. As shown in Table 2, the short-circuit current density (J_{sc}) decreased dramatically at relatively low Fc concentration, and 70% more J_{sc} was obtained in the **P1-40**/**PV** combination as compared to the **P3BT**/**PV** device. Steady-state J_{sc} for **P1-40** and **P2-40** are shown in Figure 11. Action spectra (shown in Figure 12) of the photocurrent responses covered the entire visible window (400−800 nm) for both bilayer devices under illumination from the ITO side.

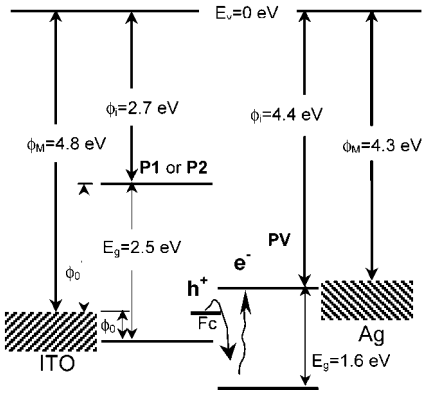

Figure 9. Energy structure of ITO/polymer/PV/Ag device. Scribble arrow represents photoexcitation in the depletion region.

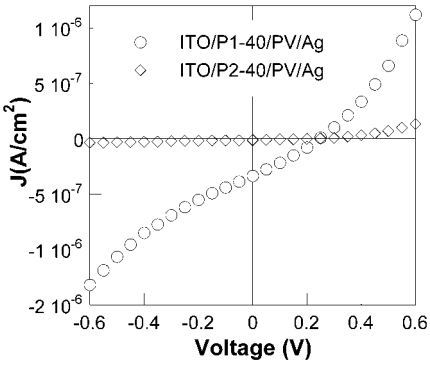

Figure 10. $J-V$ curve of polymer bilayer devices. White light was illuminated through ITO side (3.8 mW/cm^2).

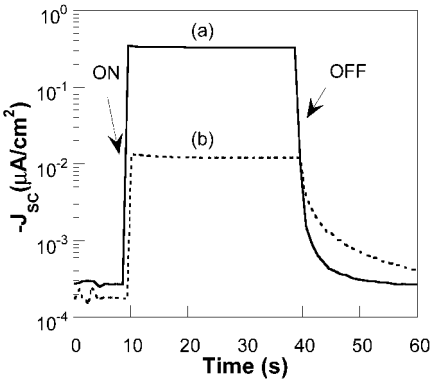

Figure 11. Steady-state short-circuit current density of polymer bilayer devices: (a) ITO/**P1-40**/**PV**/Ag; (b) ITO/**P2-40**/**PV**/Ag. White light was illuminated through ITO side (3.8 mW/cm^2).

The action spectrum in the longer wavelength region resembles the absorption spectrum of the **PV**. However, wavelengths near 2.48 eV (500 nm) appear to be more effective in producing charge carriers in relation to the shape of the **PV** absorption spectrum. Since the light arriving at the p/n junction traverses the polymer layer, we postulate that most of the light in the region, 2.5−3.1 eV (400−500) nm, is absorbed by the polymer before it reaches the p/n junction. Thus, there is little light in this spectral region available to generate carriers.[33] However, both action spectra demonstrate that polymers can be combined with **PV** to function as a solar cell over a broad wavelength range. Furthermore, we can now understand the role of the Fc group in this system. Having a higher HOMO energy level, Fc units on the p-type layer can donate electrons to the half-

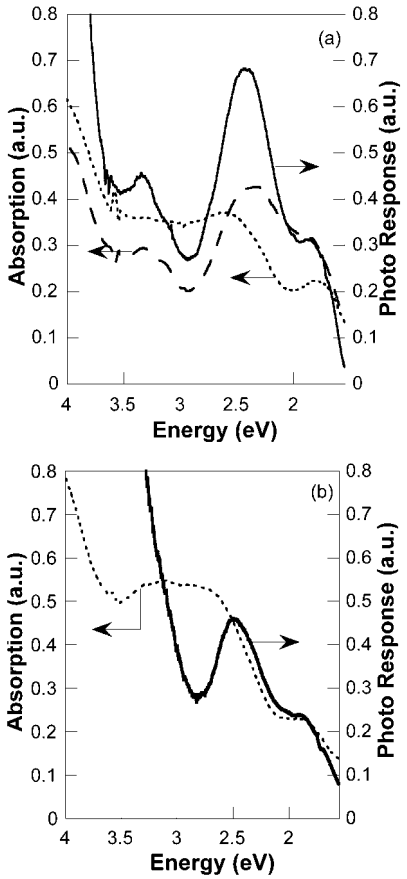

Figure 12. Action spectra of polymer bilayer device: (a) ITO/**P1-40/PV**/Ag; (b) ITO/**P2-40/PV**/Ag. White light was illuminated through ITO side (3.8 mW/cm^2). Dotted line represents optical absorption of the bilayer device, and dashed line represents UV−vis absorption of PV.

occupied HOMO of the photoexcited **PV** (or P3BT), forming Fc^+/n-doped **PV** (or P3BT) CT states. Thus, the Fc groups act as deep traps for holes by forming Fc^+, leading to a decrease in photocurrent; at high Fc concentrations, however, the hole can hop from Fc^+ to a neighboring Fc, such that, above some critical concentration, hole hopping between Fc groups becomes the dominant transport mechanism, and the photoconductivity increases.[34]

Conclusion

We have been able to show that (a) ferrocene-containing polythiophenes can be synthesized by Ni(0)-mediated copolymerization between ferrocene functionalized thiophene and brominated 3-butylthiophene, (b) there is charge transfer between the P3BT main chain and the pendant Fc groups as evidenced by the dramatic PL quenching and the spectroelectrochemistry, and (c) it is possible to fabricate organic p/n photocells using these hybrid polymers. The fabricated photocells show photoresponse over an entire visible window and dramatically increased short-circuit current density (J_{sc}) at high ferrocene concentration as compared to their parent material, P3BT.

Acknowledgment. The authors gratefully acknowledge the financial support from NSF (Grant DMR-9986123). Efficient programming on Keithley 617 by Dr. Steve Parus is gratefully acknowledged.

References and Notes

(1) Barlow, S.; Bunting, H. E.; Ringham, C.; Green, J. C.; Bublitz, G. U.; Boxer, S. G.; Perry, J. W.; Marder, S. R. *J. Am. Chem. Soc.* **1999**, *121*, 3715−3723.
(2) Southard, G. E.; Curtis, M. D. *Organometallics* **2001**, *20*, 508−522.
(3) Ching, S.; Elliott, C. M. *Langmuir* **1999**, *15*, 1491−1497.
(4) Scheytza, H.; Reissig, H.-U.; Rademacher, O. *Tetrahedron* **1999**, *55*, 4709−4720.
(5) Wang, Q.; Wang, L.; Yu, L. *J. Am. Chem. Soc.* **1998**, *120*, 12860−12868.
(6) Bäuerle, P.; Scheib, S. *Adv. Mater.* **1993**, *5*, 848−853.
(7) Park, J. Y.; Lee, S. B.; Park, Y. S.; Park, Y. W.; Lee, C. H.; Lee, J. I.; Shim, H.-K. *Appl. Phys. Lett.* **1998**, *72*, 2871−2873.
(8) Roman, L. S.; Andersson, M. R.; Yohannes, T.; Inganäs, O. *Adv. Mater.* **1997**, *9*, 1164−1168.
(9) Halls, J. J. M.; Pichler, K.; Friend, R. H.; Moratti, S. C.; Holmes, A. B. *Appl. Phys. Lett.* **1996**, *68*, 3120−3122.
(10) Kakimoto, M.; Kashihara, H.; Kashiwagi, T.; Takiguchi, T.; Ohshita, J.; Ishikawa, M. *Macromolecules* **1997**, *30*, 7816−7820.
(11) Morita, S.; Kiyomatsu, S.; Yin, X. H.; Zakhidov, A. A.; Noguchi, T.; Ohnishi, T.; Yoshino, K. *J. Appl. Phys.* **1993**, *74*, 2860−2865.
(12) Yoshino, K.; Yin, X. H.; Morita, S.; Kawai, T.; Zakhidov, A. A. *Solid State Commun.* **1993**, *85*, 85−88.
(13) Yu, G.; Pakbaz, K.; Heeger, A. J. *Appl. Phys. Lett.* **1994**, *64*, 3422−3424.
(14) Horowitz, G. *Adv. Mater.* **1990**, *2*, 287−292.
(15) Tang, C. W. *Appl. Phys. Lett.* **1986**, *48*, 183−185.
(16) Silinsh, E. A.; Kolesnikov, V. A.; Muzikante, I. J.; Balode, D. R. *Phys. Status Solidi B* **1982**, *113*, 379−393.
(17) Forrest, S. R. *IEEE J. Selected Top. Quantum Electron.* **2000**, *6*, 1072−1083.
(18) Halls, J. J. M.; Cornil, J.; dos Santos, D. A.; Silbey, R.; Hwang, D.-H.; Holmes, A. B.; Brédas, J. L.; Friend, R. H. *Phys. Rev. B* **1999**, *60*, 5721−5727.
(19) Higgins, S. J.; Jones, C. L.; Francis, S. M. *Synth. Met.* **1999**, *98*, 211−214.
(20) Naka, K.; Uemura, T.; Chujo, Y. *Macromolecules* **2000**, *33*, 6965−6969.
(21) Zhu, Y.; Wolf, M. O. *J. Am. Chem. Soc.* **2000**, *122*, 10121−10125.
(22) Pham, C. V.; Mark, H. B., Jr.; Zimmer, H. *Synth. Commun.* **1986**, *16*, 689−696.
(23) Garreau, R.; Roncali, J.; Garnier, F.; Lemaire, M. *J. Chim. Phys.* **1989**, *86*, 93−98.
(24) McCullough, R. D.; Lowe, R. D. *J. Chem. Soc., Chem. Commun.* **1992**, 70−72.
(25) Chen, T.-A.; Wu, X.; Rieke, R. D. *J. Am. Chem. Soc.* **1995**, *117*, 233−244.
(26) Ribou, A.; Launay, J.; Sachtleben, M. L.; Li, J.; Spangler, C. W. *Inorg. Chem.* **1996**, *35*, 3735−3740.
(27) Tashiro, K.; Kobayashi, M.; Kawai, T.; Yoshino, K. *Polymer* **1997**, *38*, 2867−2879.
(28) Politis, J. K.; Nemes, J. C.; Curtis, M. D. *J. Am. Chem. Soc.* **2001**, *123*, 2537−2547.
(29) Goodall, D. M.; Roberts, D. R. *J. Chem. Educ.* **1985**, *62*, 711−714.
(30) Maki, T.; Hashimoto, H. *Bull. Chem. Soc. Jpn.* **1952**, *25*, 411−413.
(31) Wu, C.-C.; Sturm, J. C.; Register, R. A.; Tian, J.; Pana, E. P.; Thompson, M. E. *IEEE Trans. Electron Devices* **1997**, *44*, 1269−1281.
(32) Hiramoto, M.; Fukusumi, H.; Yokoyama, M. *Appl. Phys. Lett.* **1992**, *61*, 2580−2582.
(33) Tan, L.; Francis, A. H.; Curtis, M. D., to be published.
(34) Zotti, G.; Zecchin, S.; Schiavon, G.; Berlin, A.; Pagani, G.; Canavesi, A. *Chem. Mater.* **1995**, *7*, 2309−2315.

MA012183V